Original Article

JOURNAL OF REINFORCED PLASTICS & COMPOSITES

Journal of Reinforced Plastics and Composites
2015, Vol. 34(14) 1113–1125

DOI: 10.1177/0731684415587346
jrp.sagepub.com

SAGE

Stiffness prediction of multilayer-connected biaxial weft-knitted fabric-reinforced composites

Yexiong Qi[1,2], Jialu Li[1,2] and Liangsen Liu[1,2]

Abstract

Based on the representative volume element (RVE) model of single layer in multilayer-connected biaxial weft-knitted (MBWK) fabric-reinforced composites, the elastic properties of multilayer-connected biaxial weft-knitted fabric-reinforced composites have been developed and presented hereafter. The average stiffness matrix of the multilayer-connected biaxial weft-knitted fabric-reinforced composites, taking into account the contribution the final geometrical of the knitting loops, can be obtained by the volume average stiffness of the unidirectional composites with different local coordinate system, and the engineering elastic constants of this kind of composites have been figured out. Numerical predictions have compared to the results of tensile tests performed on composite samples. The percentage error of the numerical prediction results and the experimental results is less than 10%.

Keywords

Multilayer-connected biaxial weft-knitted fabrics, knitted loops, representative volume element, stiffness, tensile test, classical laminate theory

Introduction

The non-crimp fabric (NCF)-reinforced composites, owning excellent in-plane[1–5] and out-of-plane properties[2,6–9] and low-manufacturing cost, have now increasing proportion in the field of aerospace, individual protection, automobile manufacturing, sporting goods, architectural engineering and medical treatment. All the time, the experimental researches[3,8,10] and theoretical analysis of the NCF-reinforced composites have been conducted for the purpose of low-cost and large-scale production. Unfortunately, the breakage of fiber has happened, because of the penetration of the needle in the process of NCFs production, which greatly affects the in-plane properties of the NCF-reinforced composites. Preventing the damage of fibers in the process of NCFs production has become a key problem that we should pay close attention to. Moreover, as a competitive member of the NCFs family, MBWK fabrics not only inherit the excellent performance of NCFs but also avoid fibers damaged in the process of knitting. In addition, the superior formability on the complex surface[11–13] has made them more popular in the field of individual protection. Nevertheless, little information has been devoted to study the prediction of elastic constants of the MBWK fabric-reinforced composites, which has increased the manufacturing cost and production cycle of the composites.

A series of recent analyses[10,14,15] about the mechanical properties of the MBWK fabric-reinforced composites have been achieved by experimental data; however, there were few literatures on the theoretical

[1]Composites Research Institute of Tianjin Polytechnic University, Xiqing District, Tianjin, China
[2]Tianjin and Education Ministry Key Laboratory of Advanced Textile Composite Materials, Xiqing District, Tianjin, China

Corresponding author:
Jialu Li, Composites Research Institute of Tianjin Polytechnic University, No. 399, Binshui West Street, Xiqing District, Tianjin, CN 300387, China.
Email: lijialu@tjpu.edu.cn

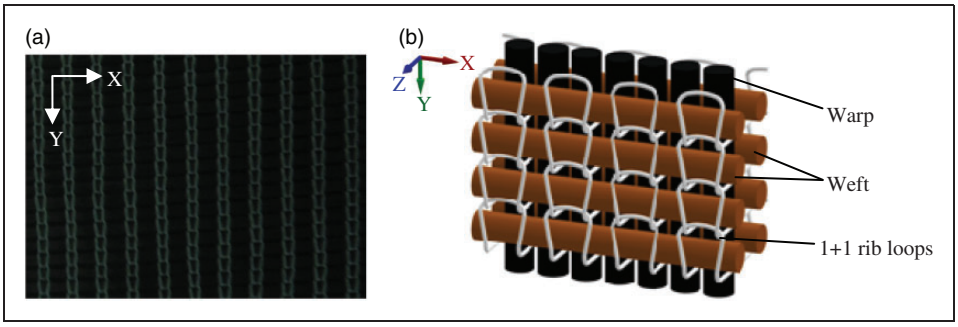

Figure 1. Structure of MBWK fabric.

analysis of the mechanical. Li and Bai[16] reported on the multidirectional tensile properties of the MBWK fabric-reinforced composites, in which the weft insertion and warp insertion consisted of glass fibers. The predicting data by the classical laminate theory (CLT) without considering bundled yarns have agreed with the experimental data, but the predicting data have been less than the experimental data, which showed that the polyester yarns have still played a certain role on the tensile properties. If we have taken into account the bundled yarns in the calculation of the CLT, the results could be better convinced. Further studies are still necessary to predict the elastic properties.

Motivated by earlier studies,[6,17,18] the main objective of this study is to present the elastic prediction method by combining the stiffness averaging method and the CLT, which put the bundled yarns into consideration, to analyze the elastic properties of the MBWK fabric-reinforced composites. More specifically, representative volume element (RVE) model is the smallest repeating unit in the single layer of multilayer-connected biaxial weft-knitted (MBWK) fabric-reinforced composites. The contribution of each single layer component (tows, bundled yarns) over the total RVE stiffness was calculated by means of stiffness averaging method. Finally, we can calculate the stiffness of MBWK fabric-reinforced composites by means of CLT. Indeed, the real benefit of this model is its capability. Due to its inherent easiness of implementation and its limited computational cost, this prediction method can be adopted throughout the different design phases, from preliminary design to detailed verification phase, taking into account the variability in material properties caused by the main geometrical sources of the MBWK fabrics. In order to verify the accuracy of the models, tensile tests of the composites structures reinforced by the MBWK fabrics are conducted in this research. The predicted results by this model showed reasonable agreements with the experimental results and proved that the model can be developed to predict the elastic properties of the MBWK fabric-reinforced composites.

In the next section, the theory behind the model is presented with considering the contribution of the knitted loops in the MBWK fabrics. The experimental activities performed on MBWK fabric-reinforced composite samples are then described. Finally, the validation activity is reported.

Modeling approach

Geometries and fibers volume fraction of RVE

As the smallest repetitive portion, the elastic properties of the RVE are representative of the global elastic properties of the single layer in MBWK fabric-reinforced composites. If we want to understand the RVE deeply and clearly, it is necessary to have a clear understanding for MBWK fabrics. The structure of MBWK fabrics is presented in Figure 1. The surface morphology of the MBWK fabrics and the schematic diagram of MBWK fabrics are also shown. The first layer of the MBWK fabric is composed of the weft yarns, the middle layer is composed of the warp yarns and the last layer is the same as the first one, all of which are bundled together as 1 + 1 rib loops by the polyester yarns (PET DTY). The MBWK fabrics were applied to produce composites with a 4-, 5- and 6-layer order lay-up (i.e. [0/90/0/90], [0/90/0/90/0] and [0/90/0/90/0/90]) to assure the different carbon fiber volume fraction. During the process of solidification, all parts in the composites had changed. The weft carbon fiber bundles shifted from the approximate circular to racetrack-shaped, the warp carbon fiber bundles shifted from the approximate circular to trapezoid and the tied polyester loops became wide and short because of pressure in the process of solidification (see Figure 2). According to above description and careful observation on the structure, the RVE of the MBWK fabric-reinforced composites is obtained as shown in Figure 3.

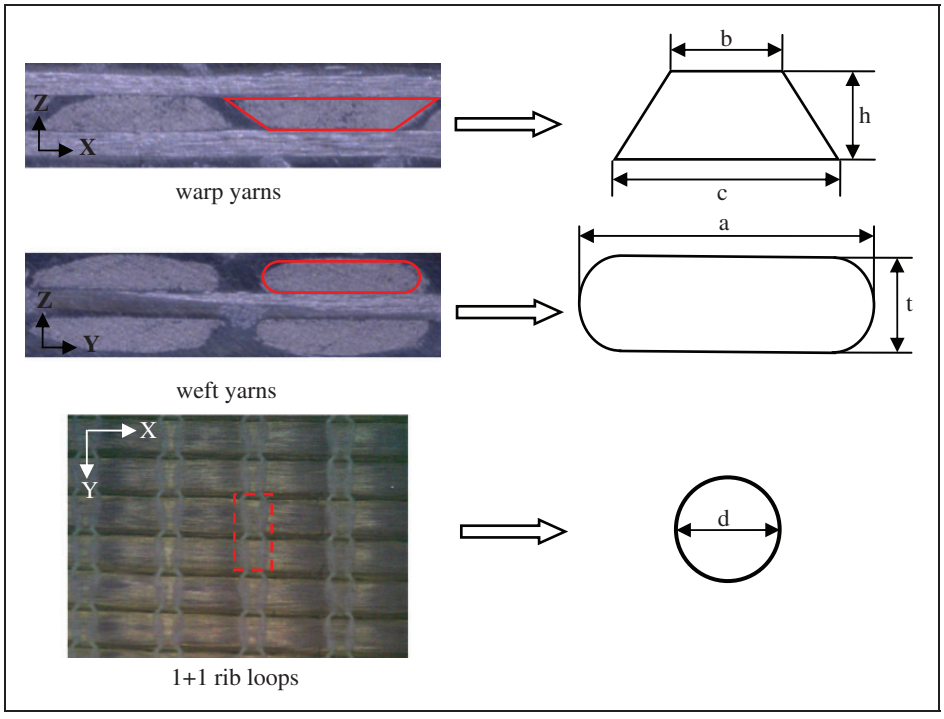

Figure 2. Cross-sections and surface morphology of MBWK fabric/epoxy composite.

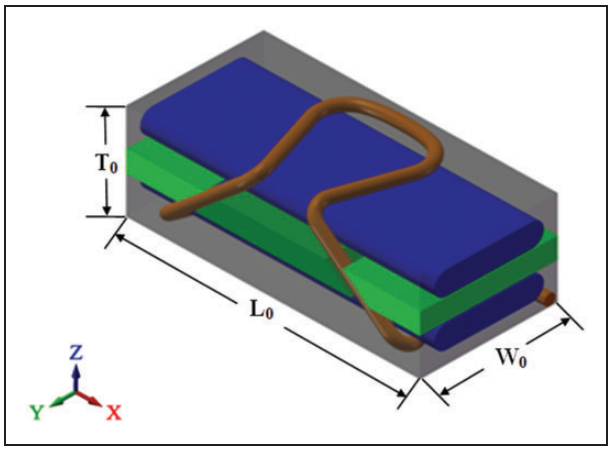

Figure 3. Repetitive volume elements with dimensions.

Figure 2 shows the microscope images of the cross-sections and surface morphology of the studied MBWK carbon fabric-reinforced composite. The path of the 1 + 1 rib loops and the compaction of weft yarns result in trapezoid warp fiber bundles cross-section instead of the approximate circular. Separately, there are few effects on the weft yarns by the path of the 1 + 1 rib loops. The main effect is the pressure in the process of solidification, as a matter of course, the weft yarns are modeled as the racetrack-shaped weft fiber bundles cross-section. Hence, the geometries of the warp and weft insertion yarns can be modeled. The geometric parameters of the fiber bundles and the RVE of the single layer are listed in Table 1, which are measured and averaged from many microscope figures. The fiber packing factor k in Table 1 is also derived from the geometric parameters and the fineness of the warp and weft fiber bundles.

Basic assumptions

Before establishing the model, four basic assumptions to simplify the analysis are made based on the observation, as listed below:

1. There are no gaps between the yarns, namely the contact between yarns is very close.
2. The yarn surface is smooth.
3. In the RVE of single layer of the MBWK fabric-reinforced composites, the first layer of the MBWK fabric is composed of the weft yarns, the middle layer is composed of the warp yarns and the last layer is the same as the first one. All material properties and geometric dimension are symmetric on the mid-plane.
4. All inserted yarns are arranged into a straight line in the composites, which is the compaction effect. The cross-section of the warp yarns is trapezoid, and the cross-section of the weft yarns is racetrack-shaped.
5. The diameter of the knitted loops cannot be ignored. The knitted loops are evenly distributed in MBWK fabric-reinforced composites.

Table 1. Geometric parameters of fiber bundles and the RVE of single layer.

Fabrics structure	Yarn	Fiber packing (%)	Dimension (mm)	Volume fraction (%)	Dimension of RVE (mm)
3l4p	Weft insertion	70.4	$b=1.17$, $c=1.84$, $h=0.22$	10.7	$L_0=4.3$
	Warp insertion	64.6	$a=1.31$, $t=0.29$	24.2	$W_0=1.9$
	Stitch	75	$d=0.14$	2	$T_0=1.0$
3l5p	Weft insertion	78.1	$b=1.32$, $c=1.81$, $h=0.19$	12.3	$L_0=4.4$
	Warp insertion	68.3	$a=1.50$, $t=0.23$	28.5	$W_0=1.9$
	Stitch	75	$d=0.14$	2	$T_0=0.85$
3l6p	Weft insertion	84.7	$b=1.37$, $c=1.92$, $h=0.17$	14.9	$L_0=4.4$
	Warp insertion	72.6	$a=1.52$, $t=0.22$	32.9	$W_0=2.0$
	Stitch	75	$d=0.14$	2	$T_0=0.7$

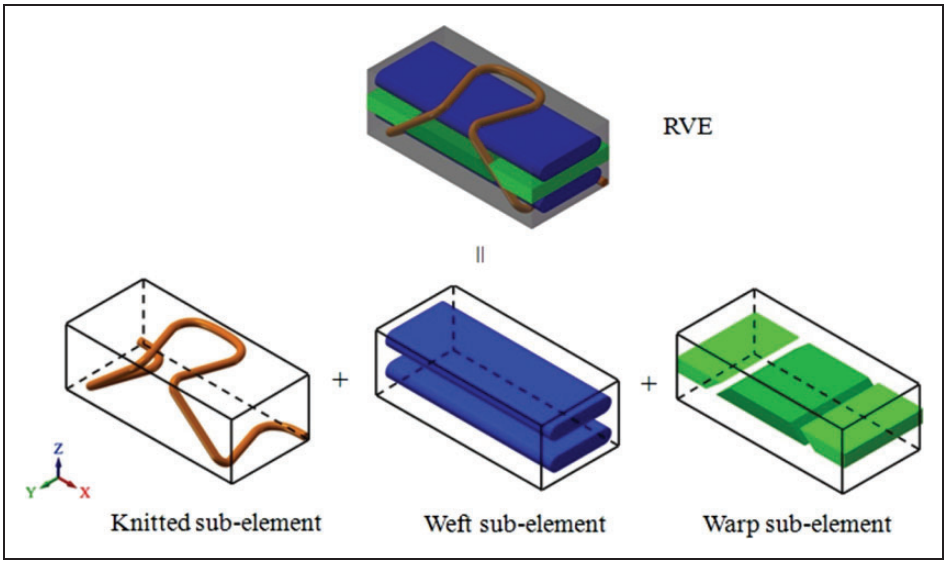

Figure 4. Decomposition sketch of the RVE.
RVE: Repetitive volume element.

Decomposition of representative volume element

For the whole single layer in the MBWK fabric-reinforced composites, the local RVE as the small microregion for the entire body keeps same averaged volume variables with global body by homogenization.[19,20] The contribution of each NCF component (warp tows, weft tows and bundled yarns) over the total RVE stiffness has been calculated by means of the stiffness averaging method. The proposed approach is based on the decomposition of the RVE into distinct sets of sub-element, respectively. Based on the structure of MBWK fabrics in the composites, the RVE of the MBWK fabric-reinforced composites is mainly divided into three parts: warp sub-element, weft sub-element and knitted sub-element. These are regarded as a separate structure. With regard to warp sub-element and weft sub-element in the RVE, a local reference system is introduced with x-axis in the fiber direction and y-axis and z-axis normal to the fiber direction. Under this assumption, the material can be considered transversely isotropic with respect to x-axis direction. The stiffness matrix can be obtained in the subsequent sections. The path of the knitted loops is complex, so each local coordinate system of tiny unit is different from global coordinate system. It is necessary to develop the mathematical model of knitted loops, which is described in detail in subsequent sections. Finally, the elastic constants of RVE can be obtained by means of collecting the analysis results of each part. The structure, separated from the RVE, is shown in the Figure 4. All sub-elements, such as warp sub-element, weft sub-element and knitted sub-element, can be analyzed by means of stiffness averaging method.

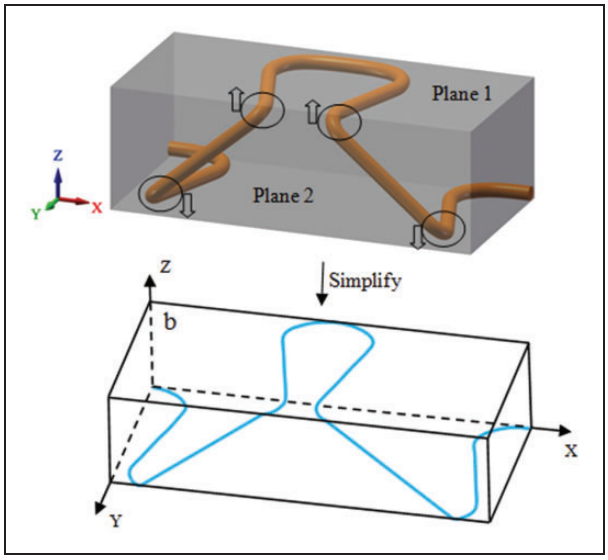

Figure 5. Simplified process of knitted loop.

Mathematical model of knitted loops

With regard to the MBWK fabric-reinforced composites, the actual three-dimensional structure of knitted loops is very complex. From plane 2 to plane 1, the yarns of the knitted loop have been distorted, such as "region a–d" (see Figure 5(a)). In this case, the establishment of the mathematical model is very difficult. In order to facilitate the mathematical analysis, the actual shape of the knitted loops has been simplified (see Figure 5(b)). The yarns in "region a" and "region d" project on the plane 2; similarly, the yarns in "region b" and "region c" project on the plane 1. On the whole, the yarns in the knitted loops distributed on three planes, which are plane 1, plane 2 and the plane perpendicular to plane 1.

Because of the uniformity and symmetry of the knitted loops, a half of the knitted loop is analyzed. As shown in Figure 6, the geometric model of knitted loops is presented. The plane "XAY" is distributing across the area of that plane where the MBWK fabrics are. The simplified knitted loop structure consists of the following several parts: top arc "AB," transition arc "BC," line segment "CD," transition arc "DE," line segment "EF," transition arc "FG," line segment "GH," transition arc "HI" and top arc "IJ". From Figure 6, we would find that, the geometrical morphology of top arc "IJ", transition arc "HI," line segment "GH," transition arc "FG" are same as the top arc "AB," the transition arc "BC," the line segment "CD," and the transition arc "DE" respectively. That is to say, they have the same mathematical equations, but they located in different locations in the space.

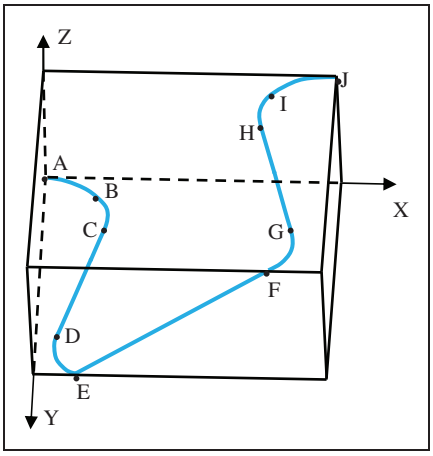

Figure 6. Geometric models of knitted loops.

Mathematical derivation of simplified curve can be used to solve the equations of the circular and liner through the knowledge of advanced mathematics. Through the known point and the relationship between each curve, the mathematical equations of the simplified knitted loop can be obtained, as follows:

$$\begin{cases} (x-0.56)^2+(y+0.07)^2=0.56^2 & x\in[0,0.22] \\ (x-0.34)^2+(y-0.22)^2=0.2^2 & x\in[0.22,0.41] \\ y=-0.26x+0.52 & x\in[0.41,1.46] \\ (x-1.54)^2+(y-0.43)^2=0.3^2 & x\in[1.46,1.80] \end{cases} \quad (1)$$

In the "XAY" coordinate system, we can get the equations of top arc "AB," transition arc "BC," line segment "CD," transition arc "DE" as shown in equation (1), in the "123" coordinate system, we can get the equation of line segment "EF" as shown in equation (2).

$$y=0.79x-0.23 \quad x\in[0.29,1.56] \quad (2)$$

Based on the geometric analysis method of the knitted loops, we can get the accurate mathematical equations of the knitted loops in the MBWK fabric-reinforced composites, which can the reasonable assurance for predicting mechanical property on the MBWK fabric-reinforced composites.

The in-plane elastic constants of knitted yarn

Generally, the elastic properties of polyester fiber bundles are kept unchanged with respect to an arbitrary rotation around a given axis. In this paper, the binder yarns are defined as the transverse isotropic materials. The binder yarns, a free space curve, are divided into an infinite number of tiny segments. For each tiny

segment, let its symmetric axis (the fiber axis in the tiny segment) be x_1. The compliance matrix of the material is the same as that given by equations (3) to (5).

$$\left[S_{ij}\right] = \begin{bmatrix} [S_{ij}]_\sigma & 0 \\ 0 & [S_{ij}]_\tau \end{bmatrix} \tag{3}$$

$$[S_{ij}]_\sigma = \begin{bmatrix} S_{11} & S_{12} & S_{12} \\ S_{12} & S_{22} & S_{23} \\ S_{12} & S_{23} & S_{22} \end{bmatrix} \tag{4}$$

$$[S_{ij}]_\tau = \begin{bmatrix} 2(S_{11}-S_{12}) & 0 & 0 \\ 0 & S_{44} & 0 \\ 0 & 0 & S_{44} \end{bmatrix} \tag{5}$$

It is worth noting that the angle is existent between the local coordinate system "123" and the global coordinate system "XOY". By the previous assumptions, the cross-section shape of the polyester fiber bundles is circular. The in-plane effective elastic constants of the tiny segment NO; *i* can be calculated through the rule of mixture formulae (see Appendix) and stress–strain relationship. We can get the compliance matrix of the tiny segment $\left[S_{ij}\right]_i^{\mathrm{L}}$ in the local coordinate system "123". When the transformation is a rotation of specific angle, we can get the compliance matrix of the tiny segment $\left[S_{ij}\right]_i^{\mathrm{G}}$ in the global coordinate system "XOY," as follows.

$$[S_{ij}]_i^{\mathrm{G}} = [\mathrm{T}]\left[S_{ij}\right]_i^{\mathrm{L}}[\mathrm{T}]^{\mathrm{T}} \tag{6}$$

With, the superscript "L" and "G" are, respectively, the local coordinate system "123" and the global coordinate system "XOY". The subscript "*i*" is the tiny segment no. *i*. The orthogonal transformation matrix is obtained by

$$[\mathrm{T}] = \begin{bmatrix} \cos^2\theta & \sin^2\theta & 0 & 0 & 0 & -\cos\theta\sin\theta \\ \sin^2\theta & \cos^2\theta & 0 & 0 & 0 & \cos\theta\sin\theta \\ 0 & 0 & 1 & 0 & 0 & 0 \\ 0 & 0 & 0 & \cos\theta & \sin\theta & 0 \\ 0 & 0 & 0 & -\sin\theta & \cos\theta & 0 \\ 2\cos\theta\sin\theta & -2\cos\theta\sin\theta & 0 & 0 & 0 & \cos^2\theta-\sin^2\theta \end{bmatrix} \tag{7}$$

In the global coordinate system "XOY," the compliance matrix of the knitted loops can be obtained, as follows:

$$[S]_{\mathrm{l},xy} = \frac{1}{\mathrm{L}}\int_0^{\mathrm{L}} [S]_i^{\mathrm{G}}\mathrm{dL} \tag{8}$$

In equation (8), the length of tiny segment can be obtained, as follows

$$\mathrm{dL} = \mathrm{A_l D}d\alpha \tag{9}$$

With, "α" is the corresponding central angle of the each arc in the knitted loop curve.

The range of "α" can be obtained from the curvilinear equations in mathematical model of knitted loops. Finally, all calculations come down to calculating the central angle of each arc in the knitted loop curve. The in-plane elastic constants of the knitted loop can be obtained.

The in-plane elastic constants of inserted yarns

In accordance with the global coordinate system XYZ represented in Figure 7, the plane of the lamina is the XY-plane and Z is the through-thickness direction. The local coordinate system 123 corresponds to the actual direction of the fiber bundles. As shown in Figure 7(a), the direction is consistent between the material axis of the inserted weft yarns and the "X" axis of the global coordinate system. In the local coordinate system, the stress-strain relationship is known by the rule of the mixture formula (see Appendix). Naturally, the elastic constant of the inserted weft yarn lamina can be obtained as same as the elastic constant in the local coordinate system. The study carried out in this section aims to evaluate the compliance matrix of the inserted weft yarns. The compliance matrix of the material in the global coordinate system is the same as that given by equations (10)to (12).

$$\left[S_{ij}^{\mathrm{we}}\right] = \begin{bmatrix} [S_{ij}^{\mathrm{we}}]_\sigma & 0 \\ 0 & [S_{ij}^{\mathrm{we}}]_\tau \end{bmatrix} \tag{10}$$

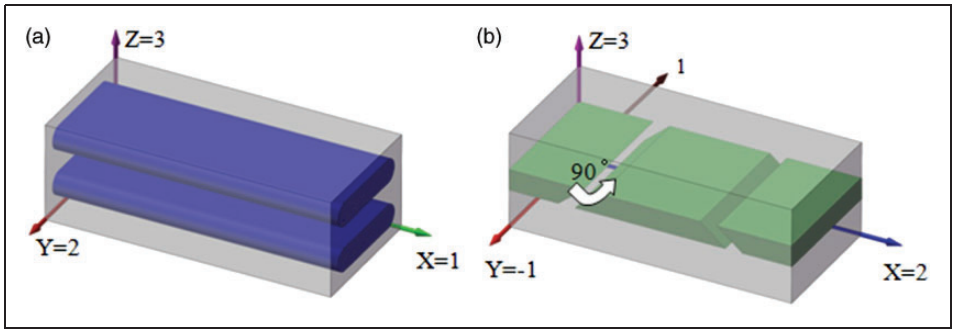

Figure 7. Relationship between material coordinate system and global coordinate system.

Table 2. Elastic properties of the tows obtained with the rule of mixtures.

	E_{11} (GPa)	E_{22} (GPa)	ν_{12}	ν_{23}	G_{12} (GPa)	G_{23} (GPa)
Fiber	220	40	0.26	–	24	14.3
Epoxy	3.5	–	0.34	–	1.23	–
Tow	198.3	16.3	0.27	0.39	6.9	8.3

$$[S_{ij}^{we}]_{\sigma} = \begin{bmatrix} S_{11} & S_{12} & S_{12} \\ S_{12} & S_{22} & S_{23} \\ S_{12} & S_{23} & S_{22} \end{bmatrix} \tag{11}$$

$$[S_{ij}^{we}]_{\tau} = \begin{bmatrix} 2(S_{11}-S_{12}) & 0 & 0 \\ 0 & S_{44} & 0 \\ 0 & 0 & S_{44} \end{bmatrix} \tag{12}$$

All of the coefficients in the matrix of equations (11) and (12) can be obtained from the rule of mixture formulae. The rule of mixture formulae has been employed as an averaging technique to estimate their values as a function of the elastic properties of the carbon fiber and of the epoxy resin (see Table 2). The epoxy resin employed is characterized by a tensile modulus $E_m = 3.50\,\text{GPa}$, a Poisson's ration $\nu_m = 0.42$ and a corresponding shear modulus $G_m = 1.23\,\text{GPa}$. Transversely isotropic carbon fibers are characterized by identical elastic properties in all planes containing the fiber axis: $E_{f11} = 230\,\text{GPa}$, $\nu_{f12} = 0.25$ and $G_{f12} = 94.8\,\text{GPa}$.

In the case of the inserted warp yarns as shown in Figure 7(b), the direction is not consistent between the material axis of the inserted warp yarns and the "X" axis of the global coordinate system. The local coordinate system can be parallel to the global coordinate system, which needs to rotate the global coordinate system along "Z" axis by 90°. Therefore, the transformation laws for the elastic compliance $[S_{ij}]_{wa}^{G}$ of the warp yarn in the global coordinate system are shown as follows:

$$[S_{ij}]_{wa}^{G} = [T][S_{ij}]_{wa}^{L}[T]^{T} \tag{13}$$

This procedure requires the use of the elastic compliance matrix of warp yarn in the local coordinate system $[S_{ij}]_{wa}^{L}$ which can be calculated from equations (14) to (16)

$$[S_{ij}]_{wa}^{L} = \begin{bmatrix} [S_{ij}^{wa}]_{\sigma} & 0 \\ 0 & [S_{ij}^{wa}]_{\tau} \end{bmatrix} \tag{14}$$

$$[S_{ij}^{wa}]_{\sigma} = \begin{bmatrix} S_{11} & S_{12} & S_{12} \\ S_{12} & S_{22} & S_{23} \\ S_{12} & S_{23} & S_{22} \end{bmatrix} \tag{15}$$

$$[S_{ij}^{wa}]_{\tau} = \begin{bmatrix} 2(S_{11}-S_{12}) & 0 & 0 \\ 0 & S_{44} & 0 \\ 0 & 0 & S_{44} \end{bmatrix} \tag{16}$$

The mechanical quantities given in the local coordinate system may have to be transformed into those in the global one or vice verse. This can be accomplished based upon the tensor transformation rules governing the stress and strain between any two rectangular coordinate systems,[21] as shown in equation (17),

$$[T] = \begin{bmatrix} 0 & 1 & 0 & 0 & 0 & 0 \\ 1 & 0 & 0 & 0 & 0 & 0 \\ 0 & 0 & 1 & 0 & 0 & 0 \\ 0 & 0 & 0 & 0 & 1 & 0 \\ 0 & 0 & 0 & -1 & 0 & 0 \\ 0 & 0 & 0 & 0 & 0 & -1 \end{bmatrix} \tag{17}$$

As aforementioned, we can obtain the elastic compliance matrix of the inserted warp yarns and weft yarns. The elastic compliance matrix of knitted loops is also obtained from the mathematical derivation of simplified curve and the tensor transformation matrix. Based on reasonable assumption, the inserted warp yarns, inserted weft yarns and the knitted loops suffer

the same stress, and the elastic compliance matrix of RVE can be combined as follows

$$[S]_{RVE,\,xy} = [S]^{w}_{i,xy}V_w + [S]^{j}_{i,xy}V_j + [S]_{l,xy}V_k \tag{18}$$

According to the relationship between the coefficient in the elastic compliance matrix of RVE and the elastic modulus of RVE, the elastic constant of the RVE of the MBWK fabric-reinforced composites can be received by the elements of the compliance matrix.

CLT prediction of elastic constants of MBWK fabric-reinforced composites

It is well known that the CLT has gained great success in composite analyses over the decades.[22] In MBWK fabric-reinforced composites, the thickness of single layer, which is consist of MBWK fabrics, is far less than the other plane dimensions. All single layers do not intersect with each other. In Li and Bai,[16] tensile modulus predictions using the CLT are introduced to compare with the available experimental results of the composite structures reinforced by the MBWK fabrics. The results are very ideal. Before calculating the tensile modulus, the assumption of plane stress is necessary, as follows.

1. MBWK fabric-reinforced composites are close-grained. The gaps and defects, because of processing, are neglectful. It is directly connected between the single layers.
2. The single layer is homogeneous, and each single layer in the MBWK fabric-reinforced composites has the same thickness. That is to say, the arbitrary tiny unit has the same macro mechanical parameter.
3. The normal stress on all cross-section paralleling to the mid-plane is far less than the other stress. We can approximately think each single layer is in a state of plane stress.
4. The tangential path, being perpendicular to mid-plane before deformation, is still perpendicular to the mid-plane after deformation. The length is constant before and after deformation.

On the basis of CLT, the stress–strain relations are described by the following relation

$$\{\sigma\} = \begin{bmatrix} Q_{11} & Q_{12} & 0 \\ Q_{21} & Q_{22} & 0 \\ 0 & 0 & Q_{66} \end{bmatrix}$$
$$\{\varepsilon\} = \begin{bmatrix} \frac{E_{11}}{1-\nu_{12}\nu_{21}} & \frac{\nu_{21}E_{22}}{1-\nu_{12}\nu_{21}} & 0 \\ \frac{\nu_{12}E_{11}}{1-\nu_{12}\nu_{21}} & \frac{E_{22}}{1-\nu_{12}\nu_{21}} & 0 \\ 0 & 0 & G_{12} \end{bmatrix}\{\varepsilon\} \tag{19}$$

Note that the above stress and strain components are expressed in the global coordinate system of the MBWK fabric-reinforced composites. In order to perform further analysis, the off axis coordinate system, the stiffness matrix $[Q_{ij}]$ can be written as

$$[Q_{ij}]_\theta = [T]_\theta [Q_{ij}][T]^{T}_\theta \tag{20}$$

where

$$[T]_\theta = \begin{bmatrix} \cos^2\theta & \sin^2\theta & -\sin 2\theta \\ \sin^2\theta & \cos^2\theta & \sin 2\theta \\ \sin\theta\cos\theta & -\sin\theta\cos\theta & \cos 2\theta \end{bmatrix} \tag{21}$$

is the transformation matrix from the material coordinates to the off axis coordinates, and the stress–strain relations in the global coordinate can be written as

$$\{\sigma\}_\theta = [Q_{ij}]_\theta\{\varepsilon\}_\theta \tag{22}$$

The neighboring layers are continuous along the thickness direction of the composites. Thus, these forces and moments, inflicting on the materials, must be balanced with the internal stress resultants. According to the equilibrium condition, we obtain

$$\begin{Bmatrix} dN_{xx} \\ dN_{yy} \\ dN_{xy} \\ dM_{xx} \\ dM_{yy} \\ dM_{xy} \end{Bmatrix} = \begin{bmatrix} A_{11} & A_{12} & A_{16} & 0 & 0 & 0 \\ A_{12} & A_{22} & A_{26} & 0 & 0 & 0 \\ A_{16} & A_{26} & A_{66} & 0 & 0 & 0 \\ 0 & 0 & 0 & D_{11} & D_{12} & D_{16} \\ 0 & 0 & 0 & D_{12} & D_{22} & D_{26} \\ 0 & 0 & 0 & D_{16} & D_{26} & D_{66} \end{bmatrix} \times \begin{Bmatrix} d\varepsilon^0_{xx} \\ d\varepsilon^0_{yy} \\ 2d\varepsilon^0_{xy} \\ dk^0_{xx} \\ dk^0_{yy} \\ 2dk^0_{xy} \end{Bmatrix} \tag{23}$$

With regard to the studied MBWK carbon fabric/epoxy composites, the x axis of the global coordinates is designated in the mid-plane and along the warp direction; consequently, the y axis is along the warp direction. All coefficients in the stiffness matrix can be calculated through the elastic properties of the RVE in the MBWK fabric-reinforced composites.

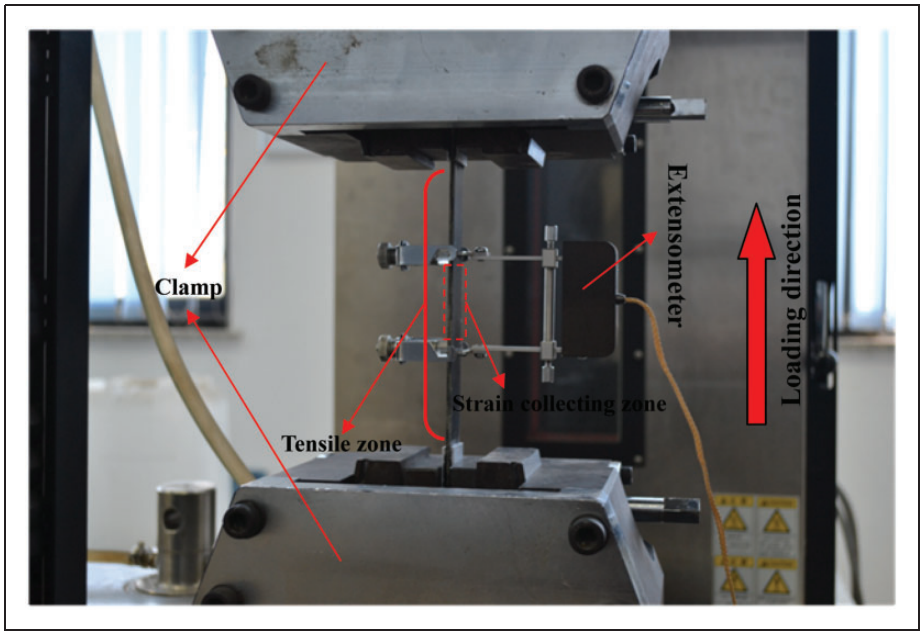

Figure 8. Tensile test setup.

Experimental details

Materials and coupons production

In this article, the MBWK fabrics, made in the Institute for Composite Materials in Tianjin Polytechnic University, were used. As shown in Figure 1, the first layer of the three-layer-connected biaxial weft knitted fabric is composed of the weft carbon fiber bundles, the middle layer is composed of the warp carbon fiber bundles and the last layer is the same as one. The weft yarns and the warp yarns, made of carbon fibers, are knitted together by the polyester yarns (PET DTY) with the 1 + 1 rib loops. The thickness of the fabric is about 1.0 mm. All composite plates were fabricated with nominal dimensions 600 mm × 360 mm × 4 mm. It is important to note that the MBWK fabrics were applied to produce composites with a 4-, 5- and 6-layer order lay-up (i.e. [0/90/0/90], [0/90/0/90/0] and [0/90/0/90/0/90]) to assure the different carbon fiber volume fraction. Each plate was characterized by the MBWK fabrics reinforcement, consolidated with epoxy resin by resin transfer molding process. The nominal dimensions of samples for the mechanical characterization have been chosen according to ASTM D3039 for tensile test.

Testing

The tensile properties of the MBWK fabric-reinforced composites are studied with 0° and 90° directional testing with different carbon fiber volume fraction. According to the structure characteristics of the samples the term of "90° samples" refers to that of the length direction of MBWK fabric-reinforced composite samples is alone the weft direction of the first piece of the samples and the term of "0° samples" refers to that the length direction of the MBWK fabric-reinforced composite samples is alone the warp direction of the first piece of the samples. The samples geometry is 250 mm × 25 mm × 4 mm, and three samples were tested in every group. 50 mm × 25 mm × 2 mm aluminum tabs are affixed to both ends of every sample on both sides. The extensometer with a gauge length of 50 mm was attached in the middle of the sample. Since the extensometer measured a large region containing a number of the textile unit cells, an overall average mechanical behavior was exhibited. And the tensile tests were conducted at the room temperature. A series of tensile tests are conducted by SHIMADZU AG-250KNE universal material testing machine in the room temperature, according to the standard of ASTM D 3039, as shown in Figure 8. In order to reduce the error of the experimental results, three specimens are evaluated for each fiber volume fraction. Since, in this paper, the carbon fiber layers of the MBWK fabric are defined as layer, the MBWK fabrics of the composite plate are defined as piece.

Results and discussion

Mechanical characterization: Tensile tests

Elastic modulus, in tensile configuration, was evaluated by linear fitting considering the stress–strain curve between $\varepsilon = 1000\,\mu\varepsilon$ and $3000\,\mu\varepsilon$. In the initial stages

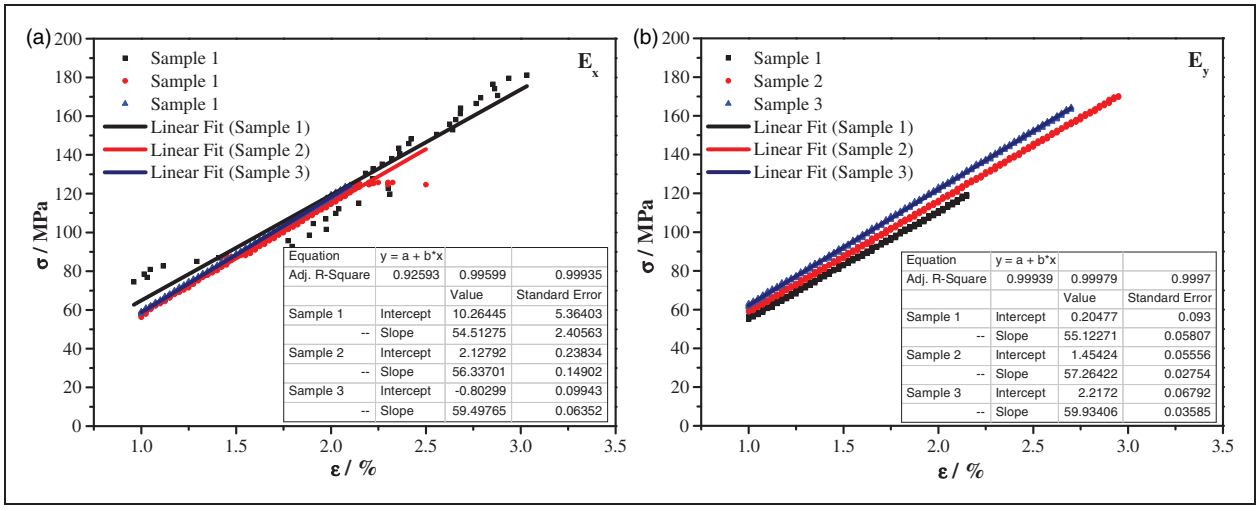

Figure 9. Experimental tensile results within the range 1000–3000 $\mu\varepsilon$ with $V_f = 33.0\%$.

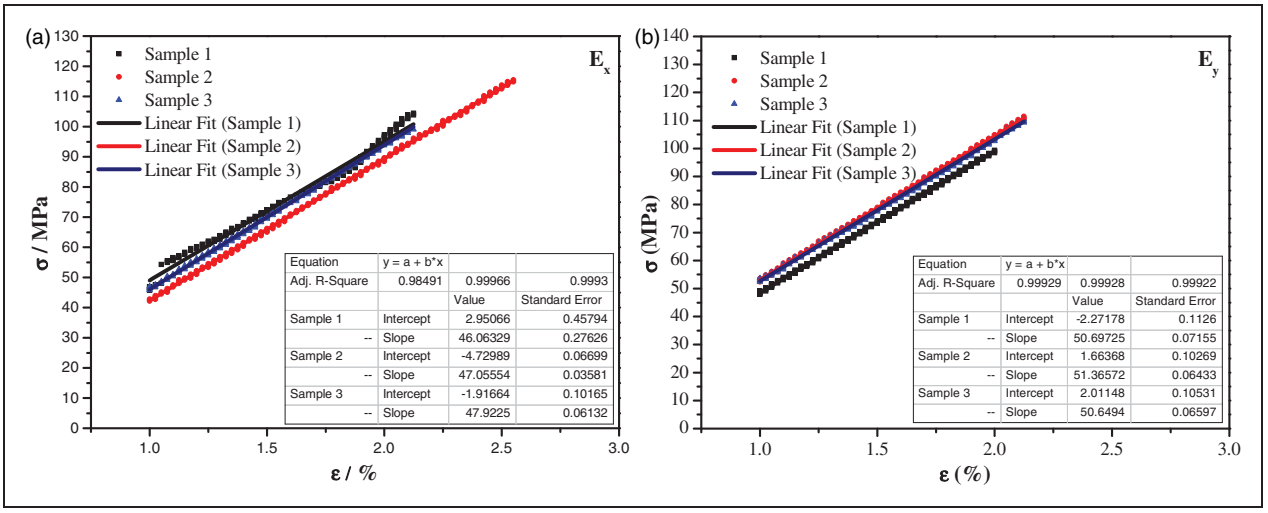

Figure 10. Experimental tensile results within the range 1000–3000 $\mu\varepsilon$ with $V_f = 39.9\%$.

of tension, surely, the composites are in the elastic range. In the stress–strain curve, evaluating the data points in the range of the $\varepsilon = 1000\,\mu\varepsilon$–$3000\,\mu\varepsilon$ by linear fitting, the slope of the stress–strain curve can be obtained. Further to say, the slope of the curve is the elastic modulus of the MBWK fabric-reinforced composites. Figures 9 to 11 show the results, respectively, for different fiber volume fraction samples tested in tensile mode, showing a repeatability of the data. Note that, all stress–strain curves have the trend of linear increasing, the linear correlation is very well. The similar conclusion has been reported earlier.[10,16] In contrast to the investigation in Rong et al.,[23] the reinforced fiber in the composites is carbon fibers rather than glass fibers. No matter which kind of fiber, carbon fiber or glass fiber, is used in the composites, the trend of linear increasing is consistent. Obviously, the results of "R" value, shown in the sheet of the Figures 9 to 11, quantitatively illuminate the linear correlation. If the "R" value is close to 1, the linear correlation is well. In other words, the size of "R" value determines the linear correlation significantly or not. For the linear fit of all samples, the "R" values are higher than 0.99. We know that all stress–strain curves have the trend of linear increasing, and there is a small difference in the same category samples, which shows that the experimental results have high reliability.

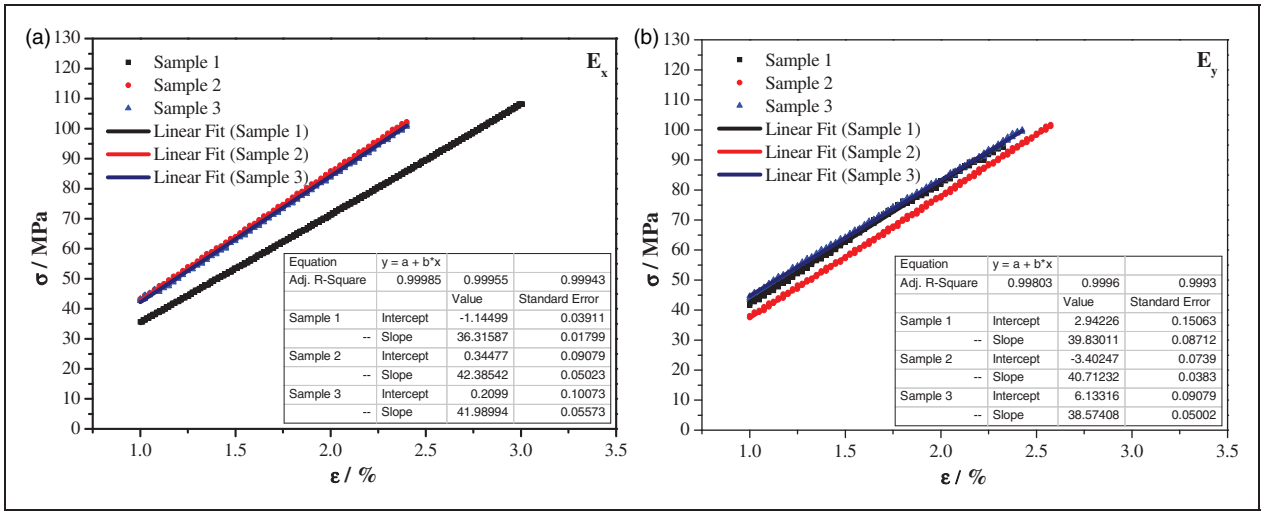

Figure 11. Experimental tensile results within the range 1000–3000 $\mu\varepsilon$ with $V_f = 48.8\%$.

Contrastive analysis of the predict results and experiment results

The elastic modulus predicted by the present model has been compared to the measured data in tension configuration for the samples described above, as shown in Figure 12. From the experimental data, we find that when the carbon fiber volume fraction in the MBWK fabrics is 33% and 48.8%, there exists a slight difference in the elastic modulus E_x and E_y, and the values are, respectively, 1.2% and 1%. Unlike above result, when the carbon fiber volume fraction in the MBWK fabrics is 39.9%, elastic modulus E_x and E_y exist obvious difference, and the corresponding values are 7.7%. The main reason for this condition is the difference of the warp yarns and weft yarns in the MBWK fabric-reinforced composite. The fiber volume fraction of the warp yarns in the MBWK fabric-reinforced composite is 18.6%; however, the fiber volume fraction of the weft yarns is 21.3%. The carbon fiber volume fraction plays the decisive role on the tensile modulus of the MBWK fabric-reinforced composites.

Another important result is that the numerical procedure results show reasonable accordance with the testing data for the tensile modulus. Numerical results were compared to the experimental data reporting the relative percentage error. The percentage error of all predicting results is less than 10%, which reveals the accuracy of the numerical procedure based on RVE of the MBWK fabric-reinforced composites. But the percentage error is different under different carbon fiber volume fraction. From Figure 12, we can see that the percentage error of the E_x and E_y, respectively, are 7.3% and 8.7%, when the carbon fiber volume fraction is 33%. The percentage error is larger than the other

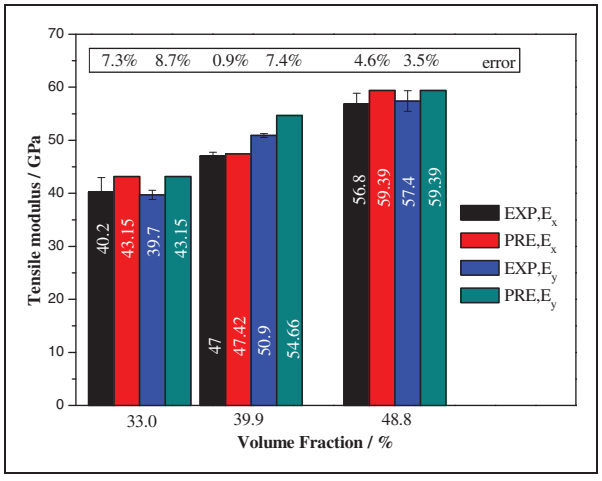

Figure 12. Experimental data vs. predictable results for the MBWK fabric-reinforced composites.

two fiber volume fraction in this research. The small percentage error of the E_x and E_y, respectively, are 4.6% and 3.5%, when the carbon fiber volume fraction is 48.8%. Separately, the percentage error of the E_x and E_y is small under the condition $V_f = 48.8\%$. It is worth that the difference of the percentage error between E_x and E_y is large under the condition $V_f = 39.9\%$. The percentage error of the E_x is 0.9%; however, the percentage error of the E_y is 7.4%. The difference of carbon fiber volume fraction caused the difference of the percentage error between the experimental results and predicting results. There are varieties of factors that cause the change of the percentage error, such as deviation of theoretical prediction, experimental error, etc. On the whole, the percentage error of all predicting results is stable and reasonable.

Additionally, the tow waviness, stitching geometrical parameters and matrix porosity, researched in earlier works,[24–27] are the main reason for the in-plane elastic properties decreasing of composites. According to the reports in the literatures, the decrease due to stitch in the composites can reach 10–20%. However, all studies tend to the negative effect on the in-plane properties of the composites, the positive influence is neglected. In this paper, the elastic modulus of knitting loops in global coordinate system can contribute positive effect. Although the contribution is little, it cannot be neglected. With respect to Figure 12, the discordance of the tensile properties is revealed by the experiment results, e.g. the modulus along the warp directions is smaller than that along the weft directions, respectively. Apart the negative effects of tow waviness, stitching geometrical parameters and matrix porosity, the contribution of the knitting loops is the main reason for this discordance of composites. In this paper, the effects of tow waviness and matrix porosity are neglected, and only the weft knitting loops is taken into consideration. If these positive factors and negative factors can be considered in the model, the predicting results will be more accurate. It also is our next target.

Conclusions

Based on the RVE model, the elastic properties of multilayer-connected biaxial weft-knitted fabric-reinforced composites have been developed and presented. The numerical procedure has been applied to predict the elastic modulus of MBWK fabric-reinforced composites. The knitting loops structure, contributing the final performance of the composites, is accounted for in the presented numerical procedure. The mathematical model of the knitting loops has been completed, which simplifies the mathematical description of MBWK fabric-reinforced composites structure. The MBWK fabric/epoxy composites have been manufactured and the tensile modulus is investigated. The predictions by the present analytical approach show a good agreement with the experiment results, which proves the practicability of the numerical procedure in the prediction of the elastic properties of MBWK fabric-reinforced composites.

Conflict of interest

None declared.

Funding

The authors wish to express their thanks to the Tianjin Municipal Science and Technology Commission for the financial supports (Grant No: 11ZCKFSF00500) that made the present study possible.

References

1. Hogg PJ, Ahmadnia A and Guild FJ. The mechanical properties of non-crimped fabric-based composites. *Composites* 1993; 24: 423–432.
2. Du GW and Frank K. Analysis of multiaxial warp-knit preforms for composite reinforcement. *Compos Sci Technol* 1996; 56: 253–260.
3. Lomov SV, Barburski M, Stoilova T, et al. Carbon composites based on multiaxial multiply stitched preforms. Part 3: biaxial tension, picture frame and compression tests of the preforms. *Compos A: Appl Sci Manuf* 2005; 36: 1188–1206.
4. Bogdanovich AE, Karahan M, Lomov SV, et al. Quasi-static tensile behavior and damage of carbon/epoxy composite reinforced with 3D non-crimp orthogonal woven fabric. *Mech Mater* 2013; 62: 14–31.
5. Drapier S and Wisnom MR. Finite-element investigation of the compressive strength of non-crimp-fabric-based composites. *Compos Sci Technol* 1999; 59: 1287–1297.
6. Liu D. Delamination resistance in stitched and unstitched composite plates subjected to impact loading. *J Reinf Plast Compos* 1990; 9: 59–69.
7. Heß H and Himmel N. Structurally stitched NCF CFRP laminates. Part 1: experimental characterization of in-plane and out-of-plane properties. *Compos Sci Technol* 2011; 71: 549–568.
8. Youjiang W, Jian L and Do PB. Properties of composite laminates reinforced with E-glass multiaxial non-crimp fabrics. *J Compos Mater* 1995; 29: 2317–2333.
9. Gan KW, Wisnom MR and Hallett SR. Effect of high through-thickness compressive stress on fibre direction tensile strength of carbon/epoxy composite laminates. *Compos Sci Technol* 2014; 90: 1–8.
10. Qi YX, Li JL and Liu LS. Tensile properties of multilayer-connected biaxial weft knitted fabric reinforced composites for carbon fibers. *Mater Design* 2014; 54: 678–685.
11. Zhang YM, Jiang YM, Qiu GX, et al. Formability of multi-layered biaxial weft knitted fabrics on double hemisphere. *J Text Res* 2005; 26: 54–56.
12. Zhang YM, Jiang YM, Qiu GX, et al. Formability ofmulti-layered biaxialweft knitted fabrics on a cylinder. *J Tianjin Polytech Univ* 2005; 24: 1–4.
13. Li XK and Bai SL. Sheet forming of the multi-layered biaxial weft knitted fabric reinforcement. Part I: on hemispherical surfaces. *Compos A: Appl Sci Manuf* 2009; 40: 766–777.
14. Wang WY, Jiang YM and Liu LS. Bending properties of multi-layered biaxial weft knitted fabric reinforced composite. *Fiber Reinf Plast* 2009; 1: 1–12.
15. Qi YX, Li JL and Liu LS. Bending properties of the multilayer-connected biaxial weft knitted fabrics-reinforced composites made with carbon fibers. *Polym Compos*. Article first published online: 5 JUL 2014. DOI: 10.1002/pc.23142.
16. Li XK and Bai SL. Tensile properties of multilayered biaxial weft knitted fabric reinforced composite material. *Plast Rubber Compos* 2010; 39: 91–98.

17. Deng Y, Chen X and Wang H. A multi-scale correlating model for predicting the mechanical properties of triaxial braided composites. *J Reinf Plast Compos* 2013; 32: 1934–1955.
18. Zrida H, Marklund E, Ayadi Z, et al. Effective stiffness of curved 0 degrees-layers for stiffness determination of cross-ply non-crimp fabric composites. *J Reinf Plast Compos* 2014; 33: 1339–1352.
19. Kanit T, Forest S, Galliet I, et al. Determination of the size of the representative volume element for random composites: statistical and numerical approach. *Int J Solids Struct* 2003; 40: 3647–3679.
20. Giannadakis K, Mannberg P, Joffe R, et al. The sources of inelastic behavior of Glass Fibre/Vinylester non-crimp fabric +/− 45 (s) laminates. *J Reinf Plast Compos* 2011; 30: 1015–1028.
21. Huang ZM and Zhou YX. *Strength of fibrous composites*, 1st ed. China: Zhejiang, 2011, p.27.
22. Huang ZM. *Introduction to micromechanics of composite materials*, 1st ed. China: Beijing, 2004, p.57.
23. Rong MZ, Zhang MQ, Liu Y, et al. Effect of stitching on in-plane and interlaminar properties of sisal/epoxy laminates. *J Compos Mater* 2002; 36: 1505–1526.
24. Riccio A and Tessitore N. A novel FEM model for biaxial non-crimp fabric composite materials under tension. *Comput Struct* 2006; 84: 1200–1207.
25. Riccio A, Zarrelli M and Tessitore N. A numerical model for delamination growth simulation in non-crimp fabric composites. *Compos Sci Tech* 2007; 67: 3345–3359.
26. Edgren F and Asp LE. Approximate analytical constitutive model for non-crimp fabric composites. *Compos A: Appl Sci Manuf* 2005; 36: 173–181.
27. Petriccione A, Annicchiarico D, Antonucci V, et al. A stiffness volume averaging based approach to model non-crimp fabric reinforced composites. *Compos Sci Tech* 2012; 72: 360–369.

Appendix

The apparent stiffness properties of the tows in the longitudinal planes (E^t_{11}, ν^t_{12} and G^t_{12}) and the transverse planes (E^t_{22}, ν^t_{23} and G^t_{23}) have been estimated from the resin stiffness properties (E^{m}, ν^{m} and G^{m}) and the stiffness properties of the fibers in the longitudinal plane (E^{f}_{11}, ν^{f}_{12} and G^{f}_{12}), using the rule of mixtures. The longitudinal elastic modulus E^t_{11}, the transverse elastic modulus E^t_{22}, the Poisson's ratio ν^t_{12}, the longitudinal shear modulus G^t_{12} and the transverse shear modulus G^t_{23} are interpolated using the following expressions

$$\begin{cases} E^t_{11} = E^f_{11} V^t_f + E^m V^t_m \\ \nu^t_{12} = \nu^f_{12} V^t_f + \nu^m V^t_m \\ E^t_{22} = \frac{E^m}{1 - V_f(1 - E^m/E^f_{22})} \\ G^t_{12} = G^t_{13} = \frac{G^f_{12} G^m}{G^f_{12} V^t_m + G^m V^t_f} \\ G^t_{23} = \frac{G^m}{1 - V_f(1 - G^m/G^f_{23})} \end{cases} \tag{A.1}$$

With, V^t_f and V^t_m being, respectively, the fiber and matrix volume fraction in the tow.